A combined analytical and computational approach to the structural behavior of composite tubes

Gérard-Philippe Zéhil
Faculty of Engineering
Notre Dame University - Louaize
P.O. Box: 72, Zouk Mikael, Lebanon
Email: gpzehil@ndu.edu.lb

***Abstract*—In this paper, we touch on the mechanical behavior of casing-infill composite tubes, as potential new lightweight structural elements. The axial and the torsional behavior of composite tubes of circular cross-section, comprising a casing and an infill, is addressed analytically, to develop physical insight into the mechanical interactions between these two components, in the linear range. The influence of the material parameters of the infill, relative to those of the casing, and of geometry – such as the ratio of wall-thickness to diameter of the casing – on the structural stiffness and capacity of the composite are revealed and presented in a novel graphical form. It is shown that significantly improved overall stiffness and capacity at yield can be obtained by bonding a moderately softer, but highly auxetic, infill to the casing, which highlights the need to develop new lightweight auxetic materials, without compromising their stiffness. These predictions are verified in torsion and confirmed in bending by means of suitable computational models based on the finite element method.**

***Keywords*—composite tubes, lightweight structural elements, auxetic materials, finite element method.**

I. Introduction

Composites play a key role in the ongoing race to develop new structural materials with improved characteristics for the various load bearing applications. The fundamental concept behind structural composites lies in the judicious combination of materials characterized by different and often complimentary properties, to achieve better overall performances.

From a structural perspective, relevant performance indicators include: (i) an improved structural efficiency characterized by higher stiffness-to-weight and strength-to-weight ratios, so as to satisfy conditions of deformability, serviceability, and resistance capacity, at reduced structural dimensions and weights, architectural constraints, and production costs, (ii) a higher damping to stiffness ratio, so as to improve the responses of structures to vibrations induced by dynamic loads, without compromising their structural efficiency, (iii) an improved structural safety, measured in terms of ductility, i.e. larger ratios of ultimate to yield deformations, and resistance capacities, (iv) improved application-specific performances such as resistances to fire, blasts, impacts, abrasion and shatter, cracking control, compactness, and reduced permeability, (v) an improved environmental impact, which implies a reduced consumption of energetic and material resources, an increased proportion of safe, environmental friendly, reusable or recyclable materials.

Filled tubes are generally constituted from an elongated tubular casing filled with a relatively softer material. These composites include: (i) concrete-filled, reinforced concrete-filled, prestressed concrete-filled, and expansive-cement-filled steel tubes, which are broadly used in construction (e.g. [1], [2]), (ii) concrete-filled fiber-reinforced polymer tubes, which were reported to be effective in applications such as piling, poles, highway overhead sign structures, and bridge components (e.g. [3], [4]), (iii) foam-filled aluminum, steel or composite tubes, or sandwich tubes, mainly used for energy absorption in applications involving very large deformation and high strain-rates, such as impacts (e.g. [5]–[8]), and (iv) epoxy polymer concrete-filled steel tubes, which were introduced and studied as potential earthquake resisting elements ([9]–[11]). Filled tubes take more or less advantage of the confining effect that the casing has on the infill. The differences between the mechanical properties of the two components influence the structural behavior of the composite. The compressibility of the infill, which may be seen as determined by its Poisson ratio, plays a key role in this regard.

Poisson's ratio has been the subject of an imposing number of papers, in the past two decades. Topics include: (i) general articles discussing Poisson's ratio and reviews on auxetic materials and their applications (e.g. [12]–[14]), (ii) developing techniques to produce novel substances, such as foams, with auxetic properties (e.g. [15]), (iii) developing new auxetic composites or studying composites with auxetic inclusions (e.g. [16], [17]), (iv) proposing modes of deformation and micro-mechanisms presenting auxetic behaviors (e.g. [18]–[20]), (v) developing models for auxetic behavior, such as micro-structural models, or models based on homogenization (e.g. [18], [21]), (vi) studying empty and filled cellular structures, including conventional and re-entrant honeycombs, in relation to auxetic properties, and damping (e.g. [19], [22]–[25]), (vii) studying auxetic fibers (e.g. [26], [27]), (viii) studying auxetic behavior in nanomaterials (e.g. [28]), (ix) examining specific properties of auxetic materials, such as their indentation behavior or their viscoelastic response (e.g. [29]), and (x) studying the nonlinear behavior of auxetic materials and structures, such as their buckling behavior, or their elasto-plastic behavior (e.g. [30], [31]). Materials with negative Poisson ratios remain at the center of many current research projects.

This work adopts a combined analytical and computational approach to reveal the influence of dimensionless material and geometric parameters on the structural efficiency of casing-infill composite tubes. It is for instance shown that significantly stiffer and stronger members can be obtained by filling the casing with a moderately softer, but highly auxetic, material.

II. Analytical approach for the axial behavior of casing-infill composite tubes

A. The empty tube

Consider an empty tube of circular cross-section. We will often refer to this tube as the "casing". Let D designate the mean diameter of the casing and t its wall-thickness, as shown in Figure 1.

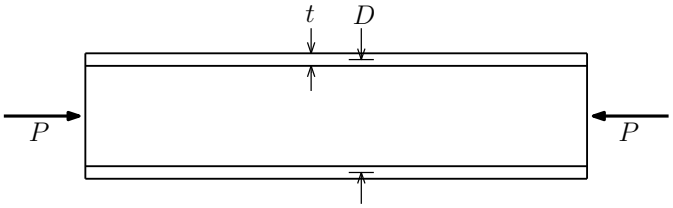

Fig. 1. Empty tube (casing) of circular cross-section.

It is assumed that the material constituting the casing behaves linearly in the elastic range. This material is therefore characterized by its Young modulus E_c, its Poisson ratio ν_c, and its normal yield stress σ_y. In intermediate sections of the tube where the axial load P is uniformly distributed, the normalized capacity at yield is given by

$$\frac{P_y}{\sigma_y D^2} = \pi \left(\frac{t}{D}\right)\left(1 - \frac{t}{D}\right), \tag{1}$$

where P_y is the axial yield load. In the following, we will assume that the wall-thickness t is much smaller than the diameter D of the tube (i.e. $t/D \ll 1$). In this case, expression (1) reduces to

$$\frac{P_y}{\sigma_y D^2} = \pi \left(\frac{t}{D}\right). \tag{2}$$

B. The composite tube

We now assume that a solid infill is bonded to the thin-walled tube. The exact way by which the axial load P is applied at both ends of the composite element does not really matter beyond a certain distance from those ends, where contact shear stresses vanish. An intermediate section of the composite tube, away from its extremities, is shown in Figure 2. The normal tractions along the axial direction in the infill and in the casing are denoted by σ_z^f and σ_z^c, respectively.

Let q refer to the normal contact pressure between the casing and the infill. The state of stress in the bonded solid infill is homogeneous; it is given by

$$\sigma_r = \sigma_\theta = -q, \tag{3a}$$
$$\sigma_z = \sigma_z^f. \tag{3b}$$

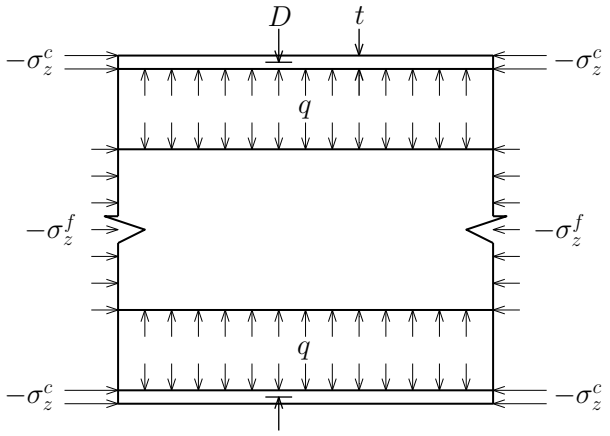

Fig. 2. Intermediate section of the composite tube.

The principal strains in the infill corresponding to those stresses write

$$\epsilon_r = \epsilon_\theta = -\frac{\nu_f}{E_f}\sigma_z^f - \frac{1-\nu_f}{E_f}q, \tag{4a}$$
$$\epsilon_z = \frac{1}{E_f}\sigma_z^f + \frac{2\nu_f}{E_f}q. \tag{4b}$$

We also write the states of stress and strain in the thin-walled casing. The principal stresses in the casing are given by

$$\sigma_r = 0, \tag{5a}$$
$$\sigma_\theta = \frac{1}{2}\left(\frac{D}{t}\right)q, \tag{5b}$$
$$\sigma_z = \sigma_z^c, \tag{5c}$$

while the principal strains resulting from those stresses are

$$\epsilon_r = -\frac{\nu_c}{E_c}\left(\frac{1}{2}\left(\frac{D}{t}\right)q + \sigma_z^c\right), \tag{6a}$$
$$\epsilon_\theta = \frac{1}{E_c}\left(\frac{1}{2}\left(\frac{D}{t}\right)q - \nu_c\sigma_z^c\right), \tag{6b}$$
$$\epsilon_z = -\frac{1}{E_c}\left(\frac{\nu_c}{2}\left(\frac{D}{t}\right)q + \sigma_z^c\right). \tag{6c}$$

The problem features three unknown quantities, i.e. q, σ_z^f and σ_z^c, and therefore requires three equations to be solved. The first equation results from the compatibility of radial displacements, or of circumferential strains, at the contact interface. Equating expressions (4a) and (6b) yields

$$\left((1-\nu_f) + \frac{1}{2}\left(\frac{E_f}{E_c}\right)\left(\frac{D}{t}\right)\right)q + \nu_f\sigma_z^f - \left(\frac{E_f}{E_c}\right)\nu_c\sigma_z^c = 0. \tag{7}$$

The second equation falls out from the compatibility of axial displacements and strains, which is due to shear bonding, at the interface between the solid infill and the casing. Equating expressions (4b) and (6c) yields

$$\left(2\nu_f + \frac{1}{2}\nu_c\left(\frac{E_f}{E_c}\right)\left(\frac{D}{t}\right)\right)q + \sigma_z^f - \left(\frac{E_f}{E_c}\right)\sigma_z^c = 0. \tag{8}$$

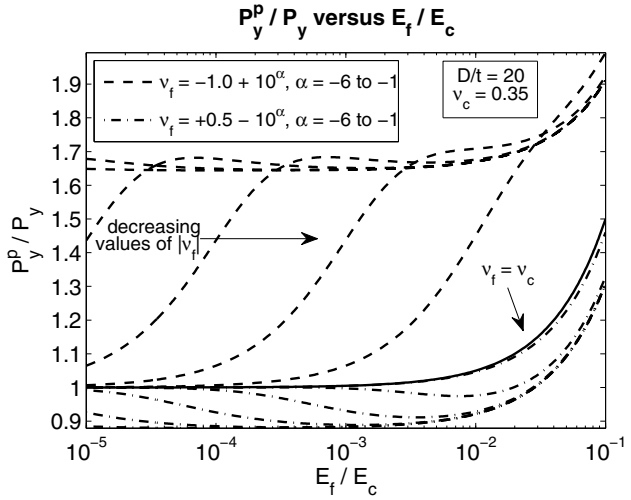

(a) P_y^p/P_y versus E_f/E_c, for $\nu_c = 0.35$ and $D/t = 20$.

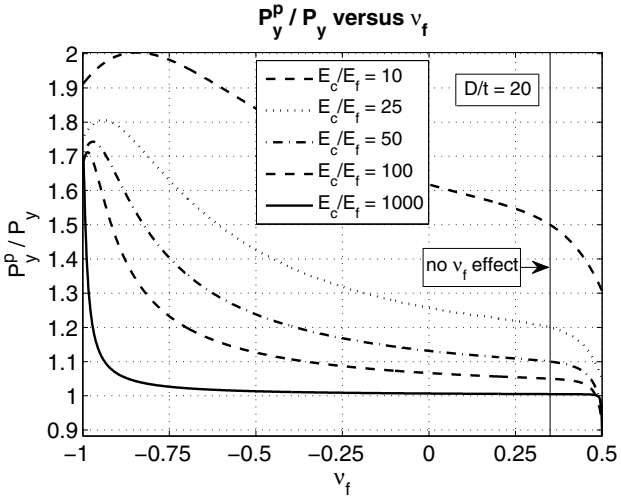

(b) P_y^p/P_y versus ν_f, for $\nu_c = 0.35$ and $D/t = 20$.

Fig. 3. Ratio of the capacity at yield P_y^p of the composite tube to the capacity at yield P_y of the casing alone.

The third equation corresponds to the equilibrium of forces in the axial direction

$$\frac{\pi D^2}{4}\sigma_z^f + \pi D t \sigma_z^c = -P. \tag{9}$$

Solving the linear system comprising equations (7), (8) and (9) for the three unknown quantities yields

$$q = \frac{8}{\pi\mathcal{B}}\left(\frac{E_f}{E_c}\right)\left(\frac{t}{D}\right)(\nu_f - \nu_c)\,\frac{P}{D^2}, \tag{10a}$$

$$\sigma_z^f = -\frac{4}{\pi\mathcal{B}}\left(\frac{E_f}{E_c}\right)\left(\left(\frac{E_f}{E_c}\right)(1-\nu_c^2) + 2\left(\frac{t}{D}\right)(1-\nu_f(1+2\nu_f))\right)\frac{P}{D^2}, \tag{10b}$$

$$\sigma_z^c = -\frac{4}{\pi\mathcal{B}}\left(\left(\frac{E_f}{E_c}\right)(1-\nu_f\nu_c) + 2\left(\frac{t}{D}\right)(1-\nu_f(1+2\nu_f))\right)\frac{P}{D^2}, \tag{10c}$$

where the dimensionless shorthand parameter $\mathcal{B}$ is given by

$$\mathcal{B} = \left(\frac{E_f}{E_c}\right)^2(1-\nu_c^2) + 2\left(\frac{E_f}{E_c}\right)\left(\frac{t}{D}\right)(3-\nu_f(1+4\nu_c)) + 8\left(\frac{t}{D}\right)^2(1-\nu_f(1+2\nu_f)). \tag{11}$$

It is noteworthy that, for a solid infill characterized by the same Poisson ratio as that of the casing ($\nu_f = \nu_c$), the normal pressure at the contact interface vanishes ($q = 0$) and the axial load is distributed between the two components proportionally to their axial stiffness, i.e. $\sigma_z^f/E_f = \sigma_z^c/E_c$.

The Von Mises yield criterion for the casing, expressed in cylindrical coordinates with $\sigma_r = 0$ (5a), writes (e.g. [32])

$$\sigma_\theta^2 + \sigma_z^2 + \sigma_\theta\sigma_z \le \sigma_y^2. \tag{12}$$

The capacity at yield P_y^p of the composite element is obtained, in normalized form, by plugging equations (10a) and (10c) into equations (5b) and (5c) and applying inequality (12) to get

$$\frac{P_y^p}{\sigma_y D^2} = \frac{\pi}{4}\frac{\mathcal{B}}{\mathcal{C}}, \tag{13}$$

where the dimensionless shorthand parameter $\mathcal{C}$ is given by

$$\mathcal{C}^2 = \left(\frac{E_f}{E_c}\right)^2\left[(1+\nu_f(1+\nu_f))(1+\nu_f^2) - \nu_c(1+\nu_f(4+\nu_f))\right] + 2\left(\frac{E_f}{E_c}\right)\left(\frac{t}{D}\right)\times (\nu_f - \nu_c + 2(1-\nu_f\nu_c))(1-\nu_f(1+2\nu_f)) + 4\left(\frac{t}{D}\right)^2(1-\nu_f(1+2\nu_f))^2. \tag{14}$$

The ratio of the axial capacity at yield P_y^p of the composite tube to the axial capacity at yield P_y of the empty casing is plotted in Figures 3a and 3b against E_f/E_c and ν_f respectively, for $\nu_c = 0.35$ and $D/t = 20$. These figures show that the best improvement in the axial capacity at yield of an empty tube can be obtained by filling the tube with a moderately soft solid material, bonded to the tube, and characterized by a strongly negative Poisson ratio (e.g. $E_f = E_c/10$ and $\nu_f \approx -0.85$). This observation reveals that sufficiently stiff and auxetic materials or meta-materials are needed. Nevertheless, it seems possible to achieve some improvement using softer infills (e.g. $E_f = E_c/1000$ and $\nu_f \to -1$). More limited results can be expected from stiffer non-auxetic infills with $\nu_f < \nu_c$. It is however important to note that, for the softer infills, the load capacity of the composite element drops very sharply as ν_f differs from -1. The high sensitivity of P_y^p to a material parameter such as ν_f may be problematic, especially as ν_f varies, for instance, with temperature, or with the level of strain.

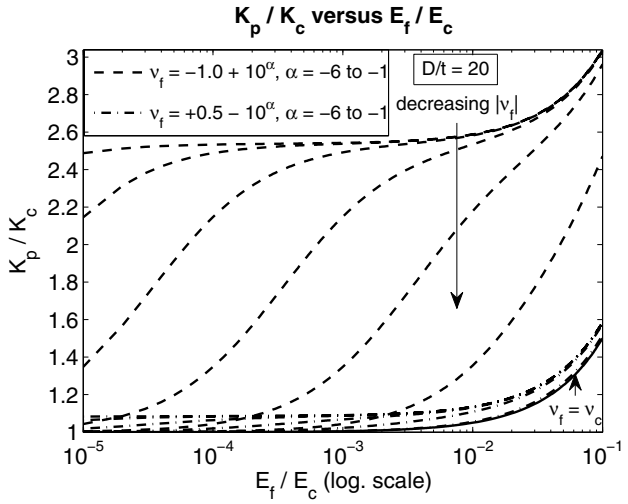

(a) K_p/K_c versus E_f/E_c, for $\nu_c = 0.35$ and $D/t = 20$.

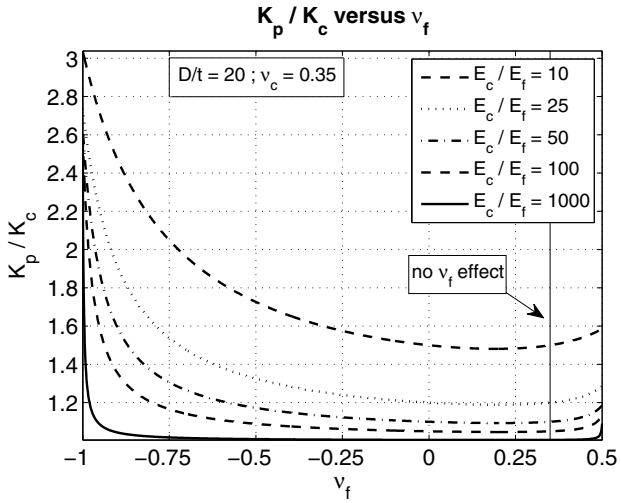

(b) K_p/K_c versus ν_f, for $\nu_c = 0.35$ and $D/t = 20$.

Fig. 4. Ratio of the axial stiffness K_p of the composite tube to the axial stiffness K_c of the empty casing.

An equivalent axial modulus E_f^{eq} for the bonded solid infill can be defined as $E_f^{eq} = \sigma_z/\epsilon_z$, where σ_z and ϵ_z are given by equations (3b) and (4b), respectively. Working out the expression of E_f^{eq} in terms of material characteristics and geometry yields

$$E_f^{eq} = \frac{E_f}{1 - \left(\frac{4\nu_f(\nu_f - \nu_c)}{2(1-\nu_f(1+2\nu_c)) + \left(\frac{E_f}{E_c}\right)\left(\frac{D}{t}\right)(1-\nu_c^2)} \right)}. \qquad (15)$$

It is worth noting that, when the bonded solid infill and the casing have the same Poisson ratio, the equivalent axial modulus of the infill is equal to its Young's modulus, i.e. $E_f^{eq} = E_f$. This is explained by the fact that, when $\nu_f = \nu_c$, there are no mechanical interactions between the two materials in intermediate sections of the composite element since, according to equation (10a), $q = 0$.

The ratio of the axial stiffness K_p of the composite tube to the axial stiffness K_c of the empty casing is readily expressed in terms of E_f^{eq}, E_c, D and t

$$\frac{K_p}{K_c} = 1 + \frac{1}{4}\left(\frac{D}{t}\right)\left(\frac{E_f^{eq}}{E_c}\right). \qquad (16)$$

The left-hand-side of equation (16) is plotted against E_f/E_c and ν_f in Figures 4a and 4b, respectively, for $\nu_c = 0.35$ and $D/t = 20$. These figures reveal that predominantly, except in the case of limited interest where $\nu_f \in [0, \nu_c]$, the ratio K_p/K_c increases with $|\nu_c - \nu_f|$, which is the greatest for highly auxetic infills. As for the capacity at yield, the axial stiffness of the composite is highly sensitive to small changes in Poisson's ratio, especially in cases where the infill is much softer than the casing. These observations further highlight the need to develop new lightweight auxetic materials without compromising their stiffness.

III. Finite element modeling in bending

A three-dimensional finite element model of a casing-infill composite tube of circular cross-section is implemented under the commercial software Abaqus to confirm that the synergistic effects predicted analytically under axial loads – mainly for auxetic infills – persist in the conditions of bending. In this numerical model, the casing of diameter $D = 30$ mm, wall thickness $t = 1.5$ mm and length $L = 450$ mm is given a Young modulus $E_c = 70$ GPa and a Poisson ratio $\nu_c = 0.35$. The material properties of the infill – E_f and ν_f – are varied to explore their influence on the ratio of the bending stiffness of the composite tube to that of the casing. The casing is modeled using quadratic, 8–node, doubly curved, thick shell elements with six degrees of freedom per node. The infill is meshed using hybrid formulation, 20–node, quadratic brick elements with linear pressure. Reduced integration is implemented to mitigate potential locking effects, especially near the incompressible limits. An average size $h = 4$ mm is retained for all elements based on a verification of convergence revealing relative changes in the outputs of less than 0.1% when h is further divided by two. The composite tube is subjected to conditions of pure bending corresponding to a maximum normal stress in the casing of $\sigma_c^{max} \approx 100$ MPa. Typical model outputs for the vertical displacement field U_2 are shown in Figures 5a and 5b corresponding to Poisson ratios $\nu_f = 0.35$ and $\nu_f = -0.99$, respectively, for $E_c/E_f = 10$. Clearly, setting $\nu_f = -0.99$ renders the composite tube roughly 2.6 times stiffer than when $\nu_f = 0.35$. This reveals that the Poisson-ratio based synergies predicted under axial loads also occur in bending. To explore the bending behavior further, many finite element simulations are run with ν_f varying between -1 and 0.5, for $E_c/E_f = 10$, 20 and 100. The numerical data points corresponding to the outputs of these simulations are interpolated and plotted in Figure 6. The trends observed in bending are very similar to those shown in

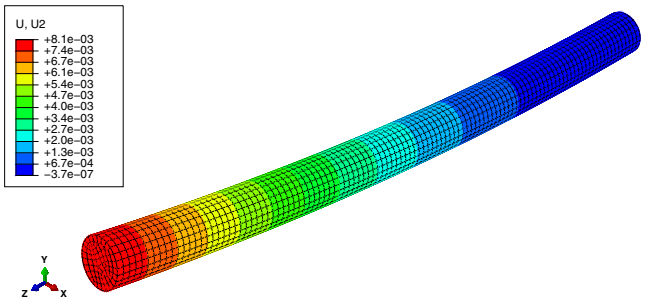

(a) $\nu_f = +0.35 \rightarrow U_2 \approx 8.1$ mm

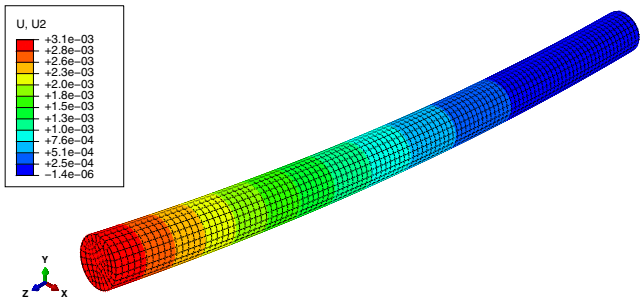

(b) $\nu_f = -0.99 \rightarrow U_2 \approx 3.1$ mm

Fig. 5. Finite element model of the composite tube with $E_c/E_f = 10$; deflection in pure bending under a moment corresponding to a maximum normal stress in the casing of 100 MPa: (a) for $\nu_f = 0.35$, and (b) for $\nu_f = -0.99$.

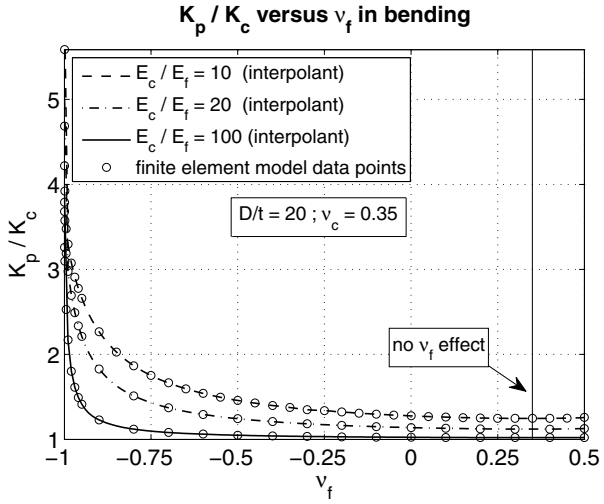

Fig. 6. Numerical results of the finite element model in pure bending: stiffness ratio K_p/K_c versus ν_f, for $\nu_c = 0.35$ and $D/t = 20$.

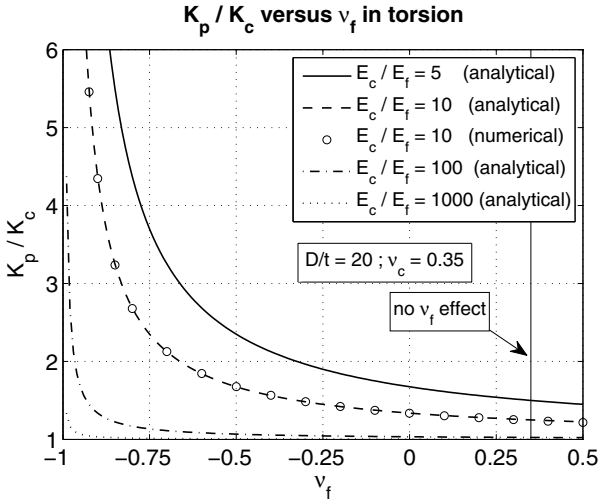

Fig. 7. Torsional stiffness ratio K_p/K_c versus ν_f, for $\nu_c = 0.35$ and $D/t = 20$. The analytical predictions perfectly match the FEM data points.

Figure 4b under axial loads: i.e (i) the best improvements in stiffness are observed with highly auxetic infills and (ii) more stable behaviors are obtained with stiffer infills.

IV. Torsional behavior

The casing-infill composite tube of circular cross-section is subjected to a torsional moment T. Due to the bonding between the casing and the infill, the angle of twist must be the same for the two components. It is thus straightforward to show that the torsional stiffness ratio K_p/K_c is given by

$$\frac{K_p}{K_c} = 1 + \left(\frac{D}{8t}\right)\left(\frac{G_f}{G_c}\right), \tag{17}$$

where $G_c = E_c/\left(2\left(1+\nu_c\right)\right)$ and $G_f = E_f/\left(2\left(1+\nu_f\right)\right)$ are the shear moduli of the casing and the infill, respectively. The variations of the stiffness ratio K_p/K_c with the Poisson ratio of the infill ν_f are plotted in Figure 7. The match between the analytical predictions obtained using equation (17) with $E_c/E_f = 10$ and numerical results was tested by running several simulations on the finite element model described in section III subjected to a pure torsional moment. Figure 7 clearly confirms that the material synergies follow a similar trend in torsion than under axial loads and bending.

V. Conclusions

To develop physical insight into the behavior of composite structural elements comprising a tubular casing and an infill, and to explore potential mechanical synergies between the materials involved, the mechanical behavior of filled circular tubes was studied and characterized in the linear range using a combined analytical and computational approach. The influences of the main, dimensionless, geometrical and material parameters on the structural performances of the composite were revealed and presented in a novel graphical form.

It was shown that significant improvements in structural stiffness and capacity at yield can be obtained by filling a relatively rigid tubular casing by a moderately softer, highly auxetic solid infill, bonded to the tube. This result emphasizes the importance of developing more auxetic materials without compromising their stiffness.

REFERENCES

[1] K. Chung, "Prediction of pre- and post-peak behavior of concrete-filled circular steel tube columns under cyclic loads using fiber element method," *Thin-Walled Structures*, vol. 48, no. 2, pp. 169 – 178, 2010. [Online]. Available: http://www.sciencedirect.com/science/article/pii/S0263823109000706

[2] Y. Deng, C. Tuan, Q. Zhou, and Y. Xiao, "Flexural strength analysis of non-post-tensioned and post-tensioned concrete-filled circular steel tubes," *Journal of Constructional Steel Research*, vol. 67, no. 2, pp. 192 – 202, 2011. [Online]. Available: http://www.sciencedirect.com/science/article/pii/S0143974X10002026

[3] I. Ahmad, Z. Zhu, and A. Mirmiran, "Behavior of short and deep beams made of concrete-filled fiber-reinforced polymer tubes," *Journal of Composites for Construction*, vol. 12, no. 1, pp. 102–110, 2008.

[4] A. Fam and S. Rizkalla, "Flexural behavior of concrete-filled fiber-reinforced polymer circular tubes," *Journal of Composites for Construction*, vol. 6, no. 2, pp. 123–132, 2002.

[5] Z. Fan, J. Shen, G. Lu, and D. Ruan, "Dynamic lateral crushing of empty and sandwich tubes," *International Journal of Impact Engineering*, vol. 53, no. 0, pp. 3 – 16, 2013, special issue based on contributions at the 3rd International Conference on Impact Loading of Lightweight Structures. [Online]. Available: http://www.sciencedirect.com/science/article/pii/S0734743X12001819

[6] A. Niknejad, H. Assaee, S. A. Elahi, and A. Golriz, "Flattening process of empty and polyurethane foam-filled e-glass/vinylester composite tubes - an experimental study," *Composite Structures*, vol. 100, no. 0, pp. 479 – 492, 2013. [Online]. Available: http://www.sciencedirect.com/science/article/pii/S0263822313000469

[7] M. Strano, A. Villa, and V. Mussi, "Design and manufacturing of anti-intrusion bars made of aluminium foam filled tubes," *International Journal of Material Forming*, vol. 6, no. 1, pp. 153–164, 2013. [Online]. Available: http://dx.doi.org/10.1007/s12289-011-1063-6

[8] S. Yang and C. Qi, "Multiobjective optimization for empty and foam-filled square columns under oblique impact loading," *International Journal of Impact Engineering*, vol. 54, no. 0, pp. 177 – 191, 2013. [Online]. Available: http://www.sciencedirect.com/science/article/pii/S0734743X12002321

[9] W. O. Oyawa, K. Sugiura, and E. Watanabe, "Polymer concrete-filled steel tubes under axial compression," *Construction and Building Materials*, vol. 15, no. 4, pp. 187 – 197, 2001. [Online]. Available: http://www.sciencedirect.com/science/article/pii/S0950061800000349

[10] ——, "Flexural response of polymer concrete filled steel beams," *Construction and Building Materials*, vol. 18, no. 6, pp. 367 – 376, 2004. [Online]. Available: http://www.sciencedirect.com/science/article/pii/S0950061804000431

[11] W. O. Oyawa, "Steel encased polymer concrete under axial compressive loading: Analytical formulations," *Construction and Building Materials*, vol. 21, no. 1, pp. 57 – 65, 2007. [Online]. Available: http://www.sciencedirect.com/science/article/pii/S0950061805002424

[12] G. N. Greaves, A. L. Greer, R. S. Lakes, and T. Rouxel, "Poisson's ratio and modern materials," *Nature Materials*, vol. 10, no. 11, pp. 823–837, 2011. [Online]. Available: http://dx.doi.org/10.1038/nmat3134

[13] Y. Liu and H. Hu, "A review on auxetic structures and polymeric materials," *Scientific Research and Essays*, vol. 5, no. 10, pp. 1052–1063, 2010. [Online]. Available: http://www.academicjournals.org/SRE

[14] Y. Prawoto, "Seeing auxetic materials from the mechanics point of view: A structural review on the negative poissons ratio," *Computational Materials Science*, vol. 58, no. 0, pp. 140 – 153, 2012. [Online]. Available: http://www.sciencedirect.com/science/article/pii/S092702561200078X

[15] D. Y. Fozdar, P. Soman, J. W. Lee, L.-H. Han, and S. Chen, "Three-dimensional polymer constructs exhibiting a tunable negative poisson's ratio," *Advanced Functional Materials*, vol. 21, no. 14, pp. 2712–2720, 2011. [Online]. Available: http://dx.doi.org/10.1002/adfm.201002022

[16] M. Assidi and J.-F. Ganghoffer, "Composites with auxetic inclusions showing both an auxetic behavior and enhancement of their mechanical properties," *Composite Structures*, vol. 94, no. 8, pp. 2373 – 2382, 2012. [Online]. Available: http://www.sciencedirect.com/science/article/pii/S0263822312000992

[17] X. Hou, H. Hu, and V. Silberschmidt, "A novel concept to develop composite structures with isotropic negative poissons ratio: Effects of random inclusions," *Composites Science and Technology*, vol. 72, no. 15, pp. 1848 – 1854, 2012. [Online]. Available: http://www.sciencedirect.com/science/article/pii/S0266353812002898

[18] J. Dirrenberger, S. Forest, D. Jeulin, and C. Colin, "Homogenization of periodic auxetic materials," *Procedia Engineering*, vol. 10, no. 0, pp. 1847 – 1852, 2011, 11th International Conference on the Mechanical Behavior of Materials (ICM11). [Online]. Available: http://www.sciencedirect.com/science/article/pii/S1877705811004954

[19] J. N. Grima, R. Cauchi, R. Gatt, and D. Attard, "Honeycomb composites with auxetic out-of-plane characteristics," *Composite Structures*, vol. 106, no. 0, pp. 150 – 159, 2013. [Online]. Available: http://www.sciencedirect.com/science/article/pii/S0263822313002869

[20] E. Pasternak and A. Dyskin, "Materials and structures with macroscopic negative poisson's ratio," *International Journal of Engineering Science*, vol. 52, no. 0, pp. 103 – 114, 2012. [Online]. Available: http://www.sciencedirect.com/science/article/pii/S0020722511002369

[21] N. Gaspar, C. W. Smith, and K. E. Evans, "Effect of heterogeneity on the elastic properties of auxetic materials," *Journal of Applied Physics*, vol. 94, no. 9, pp. 6143–6149, 2003. [Online]. Available: http://link.aip.org/link/?JAP/94/6143/1

[22] A. Alderson, K. Alderson, G. Chirima, N. Ravirala, and K. Zied, "The in-plane linear elastic constants and out-of-plane bending of 3-coordinated ligament and cylinder-ligament honeycombs," *Composites Sc ience and Technology*, vol. 70, no. 7, pp. 1034 – 1041, 2010, special issue on Chiral Smart Honeycombs. [Online]. Available: http://www.sciencedirect.com/science/article/pii/S0266353809002826

[23] M.-A. Boucher, C. Smith, F. Scarpa, R. Rajasekaran, and K. Evans, "Effective topologies for vibration damping inserts in honeycomb structures," *Composite Structures*, vol. 106, no. 0, pp. 1 – 14, 2013. [Online]. Available: http://www.sciencedirect.com/science/article/pii/S0263822313002559

[24] G. Murray, F. Gandhi, and E. Hayden, "Polymer-filled honeycombs to achieve a structural material with appreciable damping," *Journal of Intelligent Material Systems and Structures*, vol. 23, no. 6, pp. 703–718, 2012. [Online]. Available: http://jim.sagepub.com/content/23/6/703.abstract

[25] P. Soman, D. Y. Fozdar, J. W. Lee, A. Phadke, S. Varghese, and S. Chen, "A three-dimensional polymer scaffolding material exhibiting a zero poisson's ratio," *Soft Matter*, vol. 8, pp. 4946–4951, 2012. [Online]. Available: http://dx.doi.org/10.1039/C2SM07354D

[26] K. L. Alderson, V. R. Simkins, V. L. Coenen, P. J. Davies, A. Alderson, and K. E. Evans, "How to make auxetic fibre reinforced composites," *physica status solidi (b)*, vol. 242, no. 3, pp. 509–518, 2005. [Online]. Available: http://dx.doi.org/10.1002/pssb.200460371

[27] V. Simkins, A. Alderson, P. Davies, and K. Alderson, "Single fibre pullout tests on auxetic polymeric fibres," *Journal of Materials Science*, vol. 40, no. 16, pp. 4355–4364, 2005. [Online]. Available: http://dx.doi.org/10.1007/s10853-005-2829-3

[28] L. J. Hall, V. R. Coluci, D. S. Galvo, M. E. Kozlov, M. Zhang, S. O. Dantas, and R. H. Baughman, "Sign change of poisson's ratio for carbon nanotube sheets," *Science*, vol. 320, no. 5875, pp. 504–507, 2008. [Online]. Available: http://www.sciencemag.org/content/320/5875/504.abstract

[29] F. Scarpa, J. Giacomin, Y. Zhang, and P. P., "Mechanical performance of auxetic polyurethane foam for antivibration glove applications," *Cellular Polymers*, vol. 24, no. 5, pp. 253–268, 2005. [Online]. Available: http://bura.brunel.ac.uk/handle/2438/1295

[30] J. Dirrenberger, S. Forest, and D. Jeulin, "Elastoplasticity of auxetic materials," *Computational Materials Science*, vol. 64, no. 0, pp. 57 – 61, 2012, proceedings of the 21st International Workshop on Computational Mechanics of Materials (IWCMM 21). [Online]. Available: http://www.sciencedirect.com/science/article/pii/S0927025612001838

[31] H. Obrecht, B. Rosenthal, P. Fuchs, S. Lange, and C. Marusczyk, "Buckling, postbuckling and imperfection-sensitivity: Old questions and some new answers," *Computational Mechanics*, vol. 37, no. 6, pp. 498–506, 2006. [Online]. Available: http://dx.doi.org/10.1007/s00466-005-0732-z

[32] Y. Fung and P. Tong, *Classical and Computational Solid Mechanics*, ser. Advanced Series in Engineering Science Series. World Scientific, 2001. [Online]. Available: http://www.worldscientific.com/worldscibooks/10.1142/4134